



## **Sodium Gluconate as Corrosion Inhibitor for Copper in Potable Water**

**R.Sudhakaran<sup>1\*</sup>, T.Deepa<sup>2</sup>, T.Asokan<sup>1</sup>, M.Govindaraj<sup>3</sup>, T.Kasilingam<sup>4</sup>, S. Babu<sup>1</sup> and A.Sivarajan<sup>1</sup>**

<sup>1</sup>PG & Research Department of Chemistry, Govt. Arts College, Tiruchirappalli-620 022, (Affiliated to Bharathidasan University, Tiruchirappalli, 620024), Tamil Nadu, India.

<sup>2</sup>PG & Research Department of Chemistry, Govt. Arts College, (Autonomous) Karur-5. Tamil Nadu, India. (Affiliated to Bharathidasan University, Tiruchirappalli, 620024), Tamil Nadu, India.

<sup>3</sup>Department of Chemistry, K.Ramakrishna College of Technology (Autonomous), Samayapuram, Tiruchirappalli – 621112, Tamilnadu, India

<sup>4</sup>Department of Chemistry, Sacred Heart College, Villupuram, Tamil Nadu, India. (Affiliated to Thiruvalluvar University, Vellore), TamilNadu, India

E-mail: [drrskchem@gmail.com](mailto:drrskchem@gmail.com), [sanjumjetra@gmail.com](mailto:sanjumjetra@gmail.com)

### **ABSTRACT**

*The inhibition efficiency of a sodium gluconate in controlling corrosion of copper immersed in potable water has been evaluated by the absence and presence of Zn<sup>2+</sup>. The formulation consisting of SG and Zn<sup>2+</sup> has excellent inhibition efficiency (IE). The inhibition efficiency (IE%) was found to increase with increasing the concentration of the inhibitor. Electrochemical impedance spectroscopic technique (EIS) exhibit one capacitive loop indicating that, the corrosion reaction is controlled by the charge transfer process. Polarization measurements showed that the inhibitor is of mixed type. Further, the surface analysis via scanning electron microscope (SEM), energy dispersive x-ray analysis (EDX), atomic force microscope (AFM) and water contact angle technique shows a significant improvement on the surface morphology of the copper plate. The result of water contact angle technique induced by the lotus effect in copper on the surface is superhydrophobic nature.*

**KEYWORDS:** Corrosion, Copper. Corrosion Inhibition, Surface analysis, Contact angle

Received 01.03.2022

Revised 27.03.2022

Accepted 03.04.2022

### **INTRODUCTION**

Corrosion is a prevailing destructive phenomenon in science and technology. As per literature survey, the cost due to corrosion in many countries is as high as 3-5 % of the GNP i.e. wasteful in terms of economy of any country [1-3]. This represents a huge amount of money which should have been channeled into the provision of basic social amenities in these countries. The exposures can be severe to the properties of the metals as well as age of metals also, thus lead to ritual failure of materials in service.

Among all metals, copper has been one of the most common metals used for industrial and domestic purposes due to its excellent electrical conductivity, good mechanical workability, low cost, and other relatively noble properties. A variety of environmental factors can easily cause the corrosion of copper. Thus, copper corrosion and its inhibition have attracted the attention of a number of investigators [4-8]

Copper (Cu) and copper alloys have been used from prehistoric times, and their present day importance is greater than ever before [8]. Copper is one of the most important nonferrous materials [9,10] being widely used in various industries, including water distribution networks and cooling systems [8,10]. During the last decades, copper has been intensively used in microelectronics [11], owing to its combination of excellent workability, high thermal and electrical conductivities, attractive mechanical properties over a wide range of temperatures [8], high electrical conductivity and high resistance to electro-migration, which in turn results in greater circuit reliability and markedly higher clock frequency [12]. The long term operation of Cu equipment in contact with water solutions depends to a large extent on the corrosion resistance provided by Cu passivity. The passive film on Cu is usually characterized by a duplex oxide structure with an inner cuprous oxide and an outer cupric hydroxide [13]. The corrosion resistance of Cu passivation films is strongly depends on the chemical composition of water. Copper is poorly passivated in chloride-ions containing water (fresh, brackish and seawater) [9,10]. Various types of inhibitors are frequently used in water systems to improve Cu corrosion resistance. Copper is

characterized by its high electrical and thermal conductivities and good mechanical workability [14]. The main objective of the present study is to investigate the inhibitory effects of the binary inhibitor formulation containing Zn<sup>2+</sup> with SG in corrosion protection of different metals in potable water using surface analytical techniques were also used to investigate the nature of the surface film.

## MATERIAL AND METHODS

### Materials

The composition of copper steel used for corrosion inhibition studies was (Wt %): 1.57% Zn, 0.0297% Fe, 0.0103% Ni, 0.0053% Si, 0.0087% and balance being Cu. The specimens of size 1.0cm×4.0cm×0.2cm were press cut from the copper sheet, were machined and abraded with a series of emery papers. This was followed by rinsing in acetone and bidistilled water and finally dried in air. Before any experiment, the substrates were treated as described and freshly used with no further storage. The inhibitors Zn<sup>2+</sup> and SG were used as received. A stock solution of 1000ppm of SG was prepared in bidistilled water and the desired concentration was obtained by appropriate dilution. All solutions were using potable water (Perambalur, Tamil Nadu, India). The study was carried out at room temperature. The physico-chemical parameter shown in Table 1 and molecular structure of SG is given in Fig 1.

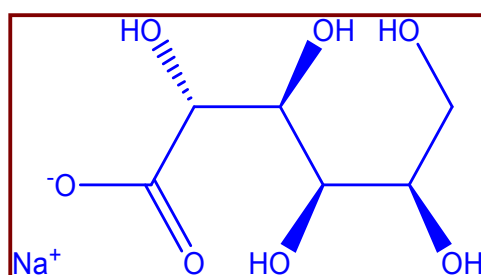


Figure 1. Molecular structure of Sodium Gluconate

Table 1. Physico-chemical parameter of potable water

| Parameters     | Values      |
|----------------|-------------|
| pH             | 7.84        |
| TDS            | 251ppm      |
| Chloride       | 30ppm       |
| Alkalinity     | 113ppm      |
| Total Hardness | 102ppm      |
| Conductivity   | 358µmhos/cm |

### Electrochemical studies

Both the potentiodynamic polarization studies and electrochemical impedance spectroscopic (EIS) studies were carried out using the electrochemical workstation model CHI-60D and the experimental data were analysed by using the electrochemical software (Version: 12.22.0.0). The measurements were conducted in a conventional three electrode cylindrical glass cell with platinum electrode as auxiliary electrode and saturated calomel electrode as reference electrode.

The working electrode was copper embedded in epoxy resin of polytetrafluoroethylene so that the flat surface of 1cm<sup>2</sup> was the only surface exposed to the electrolyte. The three electrodes set up was immersed in control solution of volume 100ml both in the absence and presence of the inhibitors formulations and allowed to attain a stable open circuit potential (OCP). The pH values of the solution were adjusted to 7.0 and the solutions were unstirred during the experiments.

Polarization curves were recorded in the potential range of -750 to -150mV with a resolution of 2mV. The curves were recorded in the dynamic scan mode with a scan rate of 2mVS<sup>-1</sup> in the current range of -20mA to +20mA. The Ohmic drop compensation has been made during the studies. The corrosion potential (E<sub>corr</sub>), corrosion current (I<sub>corr</sub>), anodic Tafel slope (β<sub>a</sub>) and cathodic Tafel slope (β<sub>c</sub>) were obtained by extrapolation of anodic and cathodic regions of the Tafel plots. The inhibition efficiency (IE<sub>p</sub>) values were calculated from the I<sub>corr</sub> values using the equation.

$$(\%) IE_p = \frac{I_{corr} - I'_{corr}}{I_{corr}} \times 100$$

Where I<sub>corr</sub> and I'<sub>corr</sub> are the corrosion current densities in case of control and inhibited solutions respectively.

Electrochemical impedance spectra in the form of Nyquist plots were recorded at OCP in the frequency range from 60KHz to 10MHz with 4 to 10 steps per decade. A sine wave, with 10mV amplitude, was used to perturb the system. The impedance parameters viz., charge transfer resistance ( $R_{ct}$ ), double layer capacitance ( $C_{dl}$ ) were obtained from the Nyquist plots. The protection efficiencies ( $IE_{im}$ ) were calculated using the equation,

$$(\%) IE_{im} = \frac{R_{ct} - R'_{ct}}{R'_{ct}} \times 100$$

Where  $R_{ct}$  and  $R'_{ct}$  are the charge transfer resistance values in the absence and presence of the inhibitor respectively.

#### Scanning electron microscope (SEM)

The mild specimen was immersed in blank and in the presence of inhibitor formulation. After seven days the specimen was taken out, washed with triple distilled water and air dried and observed in a Scanning Electron microscope examine the surface morphology. The SEM images of the surface of the specimens were obtained using VEGA3-TESCAN model in the Central Instrument Facilities. National College, Tiruchirappalli-620 002.

#### Energy Dispersive Analysis of X-ray (EDX)

EDAX (Model: BRUKER Nano Germany) system attached with Scanning Electron Microscope was used for elemental analysis or chemical characterization of the film formed on the copper. As a type of spectroscopy, it relies on the investigation of sample through interaction between electromagnetic radiation and the matter. So that, a detector was used to convert X-ray energy into voltage signals. This information was sent to a pulse processor, which measured the signals and passed them into an analyzer for data display.

#### Atomic Force Microscope (AFM)

Atomic force microscopy is a powerful method for the gathering of roughness statistics from a variety of surfaces. These exciting new techniques that allows surface to be imaged at higher resolutions and accuracies than ever before. The protective films are examined for a scanned area. AFM is becoming an accepted technique of roughness investigation [15-18]. AFM provided direct insight into the changes in the surface morphology takes place at several hundred nanometers' when topographical changes owing to the initiation of corrosion and formation of protective film on to the metal surface in the with and without addition of inhibitors respectively. All the AFM images were recorded on a Pico SPM2100 AFM instrument operating in contact mode in air. The scan size of all the AFM images are  $15\mu\text{m} \times 15\mu\text{m}$  areas at a scan rate of 0.20(Hz) lines per second.

#### Water Contact Angle

In order to evaluate the contact angle experimentally, the sessile droplet method was used. The sessile droplet rested on a horizontal substrate by a syringe. The substrate was illuminated by a light source, and then a picture was taken by using a high-resolution camera (10.1 Mpixel SONY camera). The image was processed by computer by software made for this reason.

## RESULTS AND DISCUSSION

### Potentiodynamic Polarization technique

The potentiodynamic polarization plots of copper immersed in potable water at pH 7.84 in the absence and presence of inhibitor system are shown in Figure 2. The corrosion parameters of Tafel plots are given in Table 2.

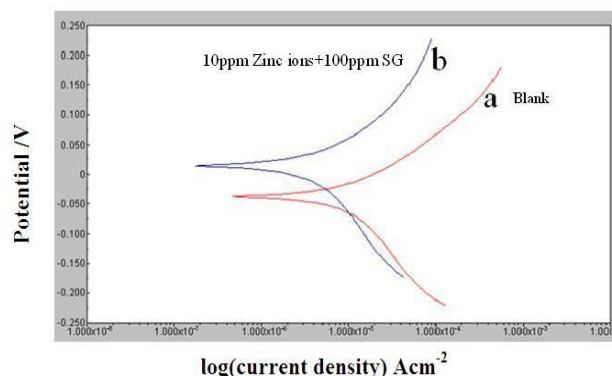


**Figure 2. Polarization curves of copper immersed in potable water in the absence and presence of inhibitors (Tafel plots)**

Various Tafel parameters, i.e., corrosion potential ( $E_{corr}$ ), corrosion current density ( $i_{corr}$ ), anodic Tafel slope ( $\beta_a$ ), cathodic Tafel slope ( $\beta_c$ ) and the inhibition efficiency ( $IE_p$ ) are given in Table 2. The results of Table 2 show that corrosion potential, ( $E_{corr}$ ) in the case of blank is  $-38\text{mV/SCE}$  and the corresponding corrosion current density ( $i_{corr}$ ) is  $6.837\text{A/cm}^2$ . The anodic Tafel slope is  $67\text{mV}$  and cathodic Tafel slope is  $119\text{mV}$ . It is clear that for the combination of  $10\text{ppm Zn}^{2+}$  and  $100\text{ppm SG}$  the corrosion potential is shifted to  $-11\text{mV/SCE}$  and its corrosion current density is also reduced, compared with the blank. Corrosion potential is slightly shifted to anodic region and the shift in anodic Tafel slope ( $69\text{mV}$ ) is greater than the shift in cathodic Tafel slope ( $108\text{mV}$ ). Corrosion potential shift  $>80\text{mV}$  suggests that the inhibitor formulation acts as mixed type inhibitor according to Ferreira, W.H. Li and C. Thangavelu [19-21]. The corrosion current is significantly decreased from  $6.837\text{A/cm}^2$  to  $0.984\text{A/cm}^2$ . The decrease in corrosion current density indicates that the rate of corrosion is minimized in the presence of  $\text{Zn}^{2+}+\text{SG}$  system due to the formation of protective film on the metal surface and the decrease in metal dissolution.

**Table 2. Corrosion parameters of copper immersed in the absence and presence of inhibitor obtained by potentiodynamic polarization studies**

| Concentration (ppm) |                  | Tafel parameters     |                                     |                     |                     | $IE_p$ (%) |
|---------------------|------------------|----------------------|-------------------------------------|---------------------|---------------------|------------|
| SG                  | $\text{Zn}^{2+}$ | $E_{corr}$ mV vs SCE | $i_{corr}$ A/cm $^2 \times 10^{-6}$ | $\beta_a$ mV/decade | $\beta_c$ mV/decade |            |
| Blank               | -                | -0.038               | 6.837                               | 67                  | 119                 | -          |
| 100                 | 10               | -0.011               | 0.984                               | 69                  | 108                 | 86         |

### Electrochemical Impedance Spectroscopic studies

Nyquist plots for the corrosion behaviour of copper immersed in potable water in the absence and presence of inhibitor system are shown in Figure 3. The impedance parameters, i.e., charge transfer resistance ( $R_{ct}$ ), double layer capacitance ( $C_{dl}$ ) and inhibition efficiency ( $IE_{imp}$ ) calculated from the Nyquist plots are given in Table 3.

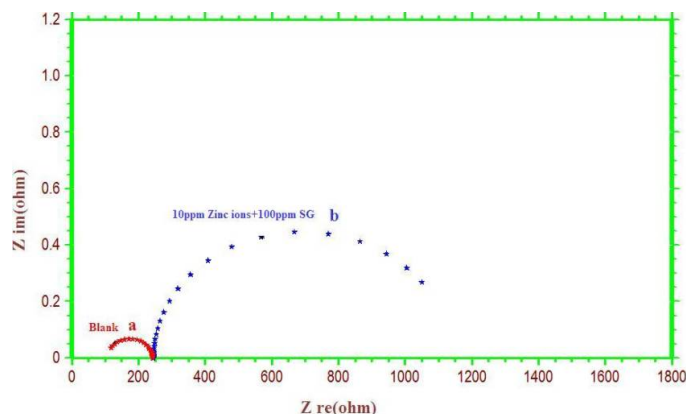


**Figure 3. Electrochemical impedance curves of copper immersed in absence and presence of inhibitors (Nyquist plots)**

**Table 3. A.C impedance parameters of copper immersed in the absence and presence of inhibitor obtained by A.C impedance spectra**

| Concentration (ppm) |                  | Charge transfer Resistance, $R_{ct}$ ( $\Omega$ ) | Double layer capacitance, $C_{dl}$ CPE $\mu\text{F/cm}^2$ | $IE_{im}$ (%) |
|---------------------|------------------|---|---|---------------|
| SG                  | $\text{Zn}^{2+}$ |   |   |               |
| Blank               | -                | 107.09  | 28.595  | -             |
| 100                 | 10               | 1104.00   | 0.262   | 90            |

The impedance diagrams obtained are not perfect semicircles and this difference has been attributed to frequency dispersion as a result of roughness in homogenates of the electrode surface [22]. The charge transfer resistance values are calculated from the difference in impedance at lower and higher frequencies, as suggested by Tsuru and Haruyama [23]. To obtain the double layer capacitance, the frequency at which the imaginary component of the impedance maximum,  $Z_{im}$  (ohm), is found and  $C_{dl}$  values are obtained from the equation:

$$f(-Z_{\max}''') = \frac{1}{2\pi C_{dl} R_{ct}}$$

The experimental data obtained from Nyquist plots are fitted by the equivalent electrical circuit shown in Figure 4.

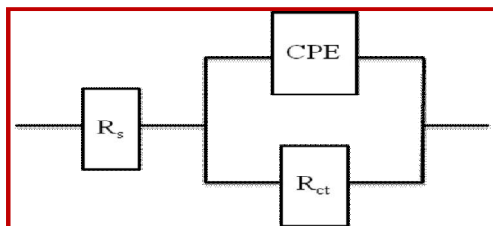


Figure 4.. Nyquist plots are fitted by the equivalent electrical circuit

Such an equivalent circuit was also discussed by several researchers who obtained similar depressed semicircles with a single time constant [24-26]. In this case, the constant phase element, CPE is introduced in the circuit instead of a pure double layer capacitor to give a more accurate fit [27].

In the present study, a small semicircle (a) with  $R_{ct}$  value of  $107.09\Omega$  is observed for the blank. When the combination of 10ppm  $Zn^{2+}$  and 100ppm SG is considered in the presence of the blank a large depressed semicircle (b) is observed from high frequency to low frequency directions in the Nyquist curves, indicating that the charge transfer resistance becomes dominant in the corrosion processes due to the presence of a protective film on the copper surface.

This result is supported by the significant decrease in  $C_{dl}$  and an increase in  $R_{ct}$  value. The semicircle obtained in the presence of  $Zn^{2+}+SG$  represents and  $R_{ct}$  value of  $1104\Omega$ , which is greater than that observed in the case of the blank (Figure 4a). A large value of  $R_{ct}$  implies a lower  $i_{corr}$  and hence, lower corrosion rate [22]. The  $C_{dl}$  value at the metal/solution interface is found to decrease from  $28.595\mu F/cm^2$  in the case of blank to  $0.262\mu F/cm^2$  in the case of the binary inhibitor formulation. The high,  $C_{dl}$  value is due to a large increase in the surface area caused by the presence of corrosion product onto the copper surface [23]. It is well known that the capacitance is inversely proportional to the thickness of the double layer [24]. Decrease in the capacitance, which can result from a decrease in the local dielectric constant and/or an increase in the thickness of the electrical double layer, strongly suggests that the inhibitor molecules are adsorbed at the metal/solution interface [25].

The value of inhibition efficiency is considerably increased in the presence of the binary inhibitor system, suggesting a decrease of in homogeneity of the interface during inhibition process. These results indicated that there is a formation of protective film in the presence of the binary inhibitor formulation. The inhibition efficiency obtained from impedance studies is found to be 90%. This is in good agreement with the inferences drawn from potentiodynamic polarization studies.

#### Scanning Electron Microscopic studies (SEM)

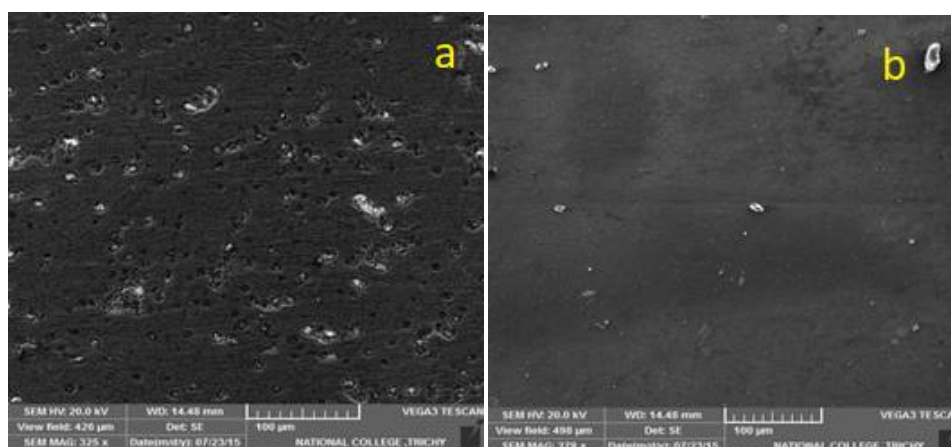


Figure 5. SEM images of copper surface immersed in a) potable water (blank) b) 10ppm  $Zn^{2+}+100ppm$  SG

Scanning electron microscopy (SEM) was analyzed to study the surface morphology of the copper immersed in the absence and presence of inhibitor formulations. Figures 5a and Figure 5b show SEM images of copper surface immersed in the absence and the presence of the inhibitor formulation respectively. It could be seen from Figure 5a ( $100\mu m$ ) reveal that the surface is strongly damaged, fault

the metallic properties and there is formation of different forms of corrosion products on the surface in the absence of the inhibitor formulation. It further shows that the corrosion products appear very uneven and the surface layer is too rough. Figure 5b (100 $\mu$ m) reveal that SEM image of polished copper immersed in the inhibitor solution are in good conditions having smooth surfaces.

It is important to stress that when the inhibitor is present in the solution, the morphology of the copper surface are quite different from the previous one. It is noted that the formation of a protective film, which is uniformly distributed on the whole surface of the metal. This may be interpreted as due to the adsorption of the inhibitor on the metal surface incorporating into the passive film in order to block the active site present on the copper surface. Thus, the protective film covers the entire metal surface. This observation also accounts for the high inhibition efficiency values obtained during the polarization studies of the inhibitor system. This indicated that the inhibitor molecules hindered the dissolution of iron by forming a protective film on the copper surface and thereby reduced the corrosion rate. So, SEM analysis shows the protective nature of the surface film [28].

### Energy Dispersive X-ray Analysis (EDX)

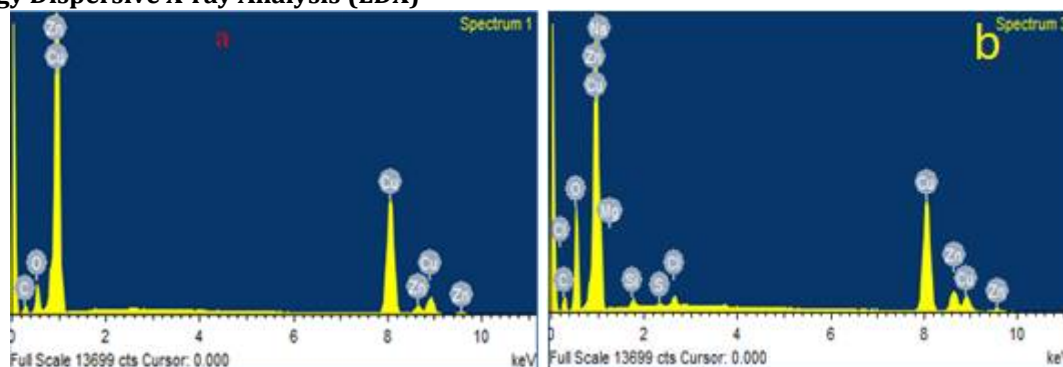


**Figure 6. EDX images of copper surface immersed in a) potable water (blank) b) 10ppm Zn<sup>2+</sup>+100ppm SG**

The composition of protective film formed on the copper surface was analyzed using EDX as shown in Figure 6a and Figure 6b. The EDX spectrum of copper sample immersed in potable water absence of inhibitor molecules was failed because it is severely weakened due to the corrosion as shown in Figure 6a. Figure 6b shows the spectrum of the system containing 10ppm Zn<sup>2+</sup>+100ppm SG. The decrease of copper peak and appearance of carbon, oxygen, sodium and zinc peak was observed due to the formation of a strong protective film of the inhibitor molecules on the surface of copper sample [29]. The action of inhibitor is related to adsorption and formation of a barrier film on the electrode surface. The formation of such a barrier film is confirmed by SEM and EDX examination of copper surface.

### Atomic Force Microscopic studies (AFM)

Atomic force microscopy (AFM) is a very high resolution type of scanning probe and it is considered to one of the most powerful techniques to investigate surface morphology. AFM is a powerful technique to investigate the surface morphology at nano to micro-scale and has become a new choice to study the influence of inhibitors on the generation and the progress of the corrosion at the metal/solution interface [30]. The topography of the surfaces recorded in 2D and 3D images was examined and surface roughness (RRMS), average roughness (Ra), maximum peak to valley height were determined from the respective images. Table 4 shows various AFM parameters obtained for the copper surface immersed in different environments. Figure 7a is observed after immersion in the blank in the absence of the inhibitor, with an increased Ra value 64.5nm (RRMS) value 88.6nm and maximum peak to valley height value of 163.2nm, indicating the formation of copper oxides. The root-mean-square (RRMS) roughness is found to be 88.6 nm, which clearly indicates the high roughness of the corroded copper surface. The microstructure of the surface shows many smaller and larger corrosion product deposits. However, Figure 7b shows that the copper immersed in inhibitor formulation, 10ppm Zn<sup>2+</sup> and 100ppm SG showed a decreased Ra value 10.9nm.

**Table 4. AFM parameters of copper surface immersed in the absence and presence of inhibitor systems**

| Samples                            | RRMS (Rq) Roughness (nm) | Average (Ra) Roughness (nm) | Maximum Peak - to - valley Height (nm) |
|------------------------------------|--------------------------|-----------------------------|--|
| Absence of inhibitor system(blank) | 88.6                     | 64.5                        | 163.2                                  |
| Presence of inhibitor system       | 13.4                     | 10.9                        | 41.4                                   |

RRMS value of 13.4nm and maximum peak to valley height is 41.4nm, which indicates the formation of a protective film on the metal surface. The decrease in RRMS roughness from 88.6nm in the case of the blank to 13.4nm observed in the case of the inhibitor formulation, clearly infers the greater homogeneity and smoothness of the surface film produced by the inhibitor formulation and the absence of any corrosion product deposits. Further, these results are confirmed by the clearly visible differences among the optical cross section analysis. The metal surface was covered with a protective film, thereby, forming a barrier against attack by aggressive ions from the corrosive environment.

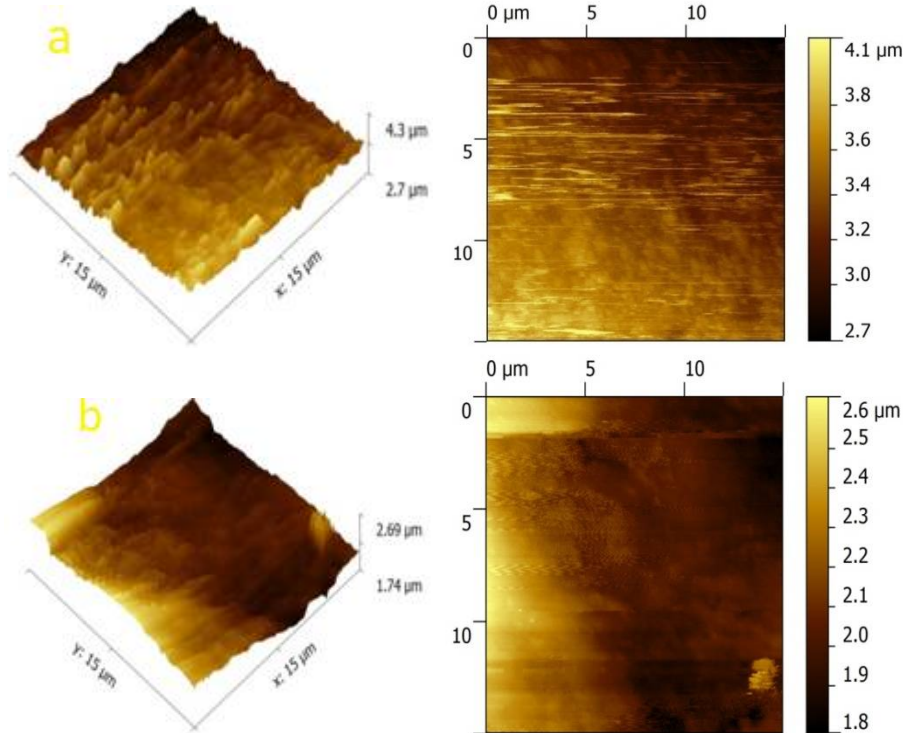


**Figure 7. AFM images of copper surface a) in potable water(blank) b) 10ppm Zn<sup>2+</sup>+100ppm SG**

#### Water Contact Angle (WCA) measurement technique

The contact angle measurement were analyzed the nature of wettability, whether it is a super hydrophobic or hydrophilic. Figure 8a shows copper surface immersed in potable water, surface highly porous, more roughness (WCA  $83^{\circ} \pm 2^{\circ}$ ) due to copper surface get hydrophilic nature. Figure 8b shows copper surface immersed in the presence of inhibitor formulation 10ppm Zn<sup>2+</sup>+100ppm SG smoother surface appear (WCA  $158^{\circ} \pm 4^{\circ}$ ) beside the surface gets super hydrophobic nature [31]. This confirms the adsorption of a super hydrophobic protective film adsorbed onto the copper surface in the presence of inhibitor molecule.

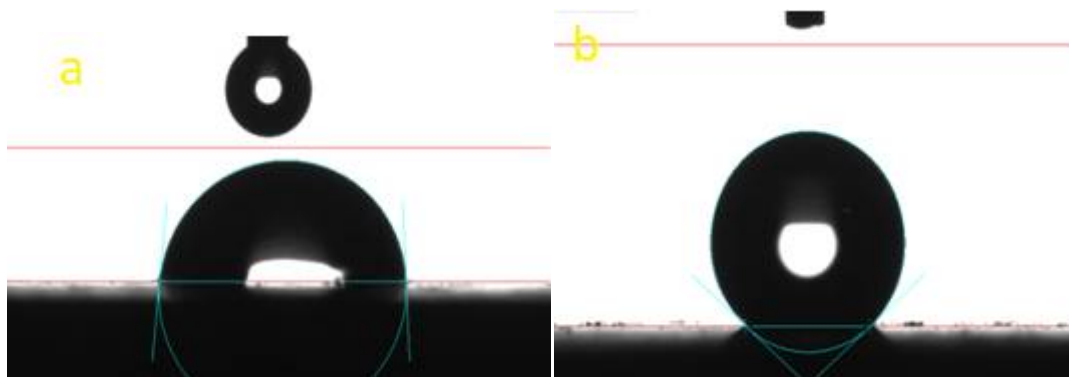


**Figure 8. WCA images of copper surface immersed in a) potable water (blank) b) 10ppm Zn<sup>2+</sup>+100ppm SG**

**CONCLUSION**

The maximum corrosion inhibition efficiency offered by the formulations consisting of 10ppm of Zn<sup>2+</sup> and 100ppm of SG was 90%. Polarization study revealed the inhibitors inhibit copper through mixed type inhibitor. Electrochemical impedance spectroscopy (EIS) results confirm the formation of protective film, which has a very high charge transfer resistance of the inhibitors at copper in potable water interface. The results of SEM and EDX images indicate the protective film formation on the surface is corroborated by AFM images of copper. Water contact angle measurements revealed the formation of a superhydrophobic nature of protective film. Based on the electrochemical studies and spectroscopic techniques, a suitable mechanism has been proposed for Zn<sup>2+</sup>+SG systems.

**REFERENCES**

1. J.J. Moore, (1994). Butterworth-Heinemann Ltd.: Boston, New Jersey, pp. 351-393,
2. M.G. Fontana, (2005). Corrosion Engineering, 2nd ed., Tata McGraw Hill: New Delhi.
3. Sharma, Alka, S. K. Sharma (Ed.) (2011). Wiley-VCH Verlag GmbH and Co. KGaA, pp.157-80.
4. E.M. Sherif, S.M. Park, (2006). *Electrochim. Acta*, 51:4665-4673. DOI <http://dx.doi.org/10.1016/j.electacta.2006.01.007>
5. S. S. A. Rehim, H. H. Hassan, and M. A. Amin, (2002). "Corrosion and corrosion inhibition of Al and some alloys in sulphate solutions containing halide ions investigated by an impedance technique," *Appl. Surf. Sci.*, **187**, 279-290
6. C.C. Yang, Mater. (1994). *Chem. Phys.*, 37:355-361.
7. M. Baumgartner, H. Kaesche, (1990). *Corros. Sci.*, 31:231-236.
8. L. Shreir, R. Jarman, G. Burstein, (1994). *Corrosion, Metal/Environment Reactions*, vol. 1, Butterworth-Heinemann, Oxford, England.
9. H.H. Strehblow, B. Titze, (1980). The investigation of the passive behaviour of copper in weakly acid and alkaline solutions and the examination of the passive film by ESCA and ISS, *Electrochim. Acta.*, 25: 839-850.
10. M. Finšgar, I. Milošev, (2010). *Corros. Sci.*, 52:2737-2749.
11. S.P. Murarka, I.V. Verner, R.J. Gutmann, S.P. Murarka, (2000). *Copper-Fundamental Mechanisms for Microelectronic Applications*, John Wiley.
12. Y. Ein-Eli, D. Starosvetsky, (2000). *Electrochim. Acta.*, 52:1825-1838.
13. L. Burke, M. Ahern, T. Ryan, J. (1990). *Electrochem. Soc.*, 137:553-561.
14. L. Nunez, E. Reguera, F. Corvo, E. Gonzalez, and C. Vazquez, (2005). *Corros. Sci.*, 47:461-484.
15. C. Amra, C. Deumie, D. Torricini, P. Roche, R. Galindo, P. Dumas, and F. Salvan (1994). *International Symposium On Optical Interference Coatings*, 6-10 June 1994. Grenoble, Proceedings. SPIE 2253,614.
16. R.N. Bhattacharyya, (1983). *Experiments with Micro Organisma* (EMKAY) Publications.
17. J. Micheal Pelczar, JREC Schan Noel R: Krieg; (1988). *Micro Biology*, Tata Magraw-Hill Education.
18. W.C. Bigelow, D.L. Pickett, W.A.J. Zisman, (1946). *Colloids Science*, 1:513.
19. Ferreira E S, Giacomellic C, Giacomellic F C, and Spinelli A, (2004). *Material Chemistry and Physics*, 83( 1):129.
20. Li W H, He Q, Pei C L and Hou B R, (2008). *Journal of Applied Electrochemistry*, 38: 3:289.
21. T Asokan and C. Thangavelu., (2014). *Journal of Advances in Chemistry*, 10( 3):2369.
22. H.H. Uhlig and R.W. Revie, (1985). *Corrosion and Corrosion Control*, 3rd edition. Wiley, New York.
23. Bonnel, F. Dabosi, C. Desloviés, M. Duprat, M. Keddam and Tribollet, (1983). *Journal of Electrochemical Society*, 3; 130:753.
24. P. Li, J.Y. Lin, K.L. Tan, J.Y. Lee, (1997). *Electrochimica Acta*, 42:605.
25. H. Zarrok, H. Oudda, El A. Midaoui, A. Zarrouk, B. Hammouti, Ebn M. Touhami, A. Attayibat, S. Radi, R. Touzani, (2012). *Research Chemical Intermed*, 38:2051.
26. B. Balanaga Karthik, P. Selvakumar and C. Thangavelu, (2014). *International Journal of Science and Research*, 4:1.
27. Chinnayan Thangavelu and Thavan Kasilingam, (2014). *Chemical Science Review Letters*, 3 (9):10.
28. B.V. AppaRao, M. VenkateswaraRao, S. SrinivasaRao, B. Sreedhar, (2010). *Journal of Chemical Science*, 122:639.
29. M.A. Amin, (2006). *Journal of Applied Electrochemistry*, 36:215.
30. A.K. Satapathy, G. Gunasekaran, S.C. Sahoo, K. Amit, P.V. Rodrigues, (2009). *Corrosion Science*, 51:2848.
31. R. Sudhakaran, S. Babu, A. Sivarajan, T. Kasilingam and T. Asokan, (2021). *Gorteria Journal*, 34:1 182-190.

**CITATION OF THIS ARTICLE**

R. Sudhakaran, T. Deepa, T. Asokan, M. Govindaraj, T. Kasilingam, S. Babu and A. Sivarajan. Sodium Gluconate as Corrosion Inhibitor for Copper in Potable Water. *Bull. Env. Pharmacol. Life Sci.*, Spl Issue [1] 2022 : 486-493